Journal of Pharmacokinetics and Biopharmaceutics, Vol. 8, No. 4, 1980

Tissue Distribution Kinetics of Tetraethylammonium Ion in the Rat

Mark Mintun,[1] Kenneth J. Himmelstein,[1] Richard L. Schroder,[2] Milo Gibaldi,[3] and Danny D. Shen[2,4]

Received October 18, 1979

Tissue distribution kinetics of tetraethylammonium (TEA) ion in rats were studied following both constant-rate intravenous infusion and rapid intravenous injection of the drug. At a steady-state plasma concentration of 0.2 μg/ml, the tissue-to-plasma (T/P) concentration ratio of the kidneys, liver, heart, gut, and lungs exceeded 1, indicating that TEA is localized in these tissues. In vitro *tissue homogenate binding and slice uptake experiments provided no evidence of TEA binding to tissue constituents, suggesting that the high T/P concentration gradient is due to an active transport process. The maximum concentration of TEA in all tissues occurred within 5–15 min after rapid injection of a 2-mg dose. Except for the liver, the subsequent decline of TEA concentration in various tissues over a 5-hr period was slow compared to that in plasma. Consequently, the T/P ratio of liver and kidney remained relatively constant, while those of the other tissues increased continually with time. These features of TEA tissue distribution kinetics can be predicted by a physiologically based pharmacokinetic model which incorporates both active and passive transport processes for the passage of TEA between blood and the tissue mass.*

KEY WORDS: tetraethylammonium ion; tissue distribution; active transport; physiological pharmacokinetic model.

INTRODUCTION

In recent years efforts have been directed toward the design of physiologically realistic pharmacokinetic models. These comprehensive models are developed on the basis of and incorporate physiological, anatomical, and physicochemical data. Previous applications of physiologically based

This work was supported in part by United States Public Health Service Grants No. GM-20852 (M. G. and D. D. S.), GM-15956 (D. D. S.), and RR-07037 (K. J. H.).

[1]Department of Chemical and Petroleum Engineering, University of Kansas, Lawrence, Kansas 66045.

[2]Present address: Department of Pharmaceutics, School of Pharmacy, University of New York at Buffalo, Amherst, New York 14260.

[3]Present address: School of Pharmacy, University of Washington, Seattle, Washington 98195.

[4] Address correspondence to D. D. S.

0090-466X/80/0800-0373$03.00/0

pharmacokinetic models to drugs and other xenobiotics have recently been reviewed by Himmelstein and Lutz (1). The utility of these models is superior in principle to that of the classical compartmental models in several respects. Ideally, they permit an exact description of the time course of drug concentration in any organ or tissue and are, therefore, able to provide much greater insight into the dynamics of drug distribution in the body. Also, since the parameters of these models correspond to actual physiological and anatomical measures such as organ blood flows and volumes, changes in the disposition kinetics of a drug due to physiological or pathological alterations in body function can often be predicted by perturbation of the appropriate parameters (2). Finally, these biologically realistic models introduce the concept of animal scale-up, which would provide a rational basis for the correlation of drug disposition data between animal species (3).

The majority of the physiological-type models developed to date are based on the assumption that drug movement within a tissue compartment is much more rapid than the rate of delivery of drug to the tissue by the perfusing blood. Under such a condition, drug distribution into various body compartments is rate-limited by blood flow. The assumption of perfusion-limited transport is applicable to highly lipid soluble and weakly ionized compounds, in which case diffusion or movement across lipoidal membranes should be relatively rapid. On the other hand, with highly polar and strongly ionized or permanently charged compounds, diffusion and/or transport across cellular membrane can be a slow step in the overall uptake process. Hence a tissue distribution model for such drugs needs to include the joint effects of blood flow and transport across cell membranes.

We have studied the tissue distribution kinetics of a cation tetraethylammonium (TEA) in the rat following rapid intravenous injection. Despite the presence of a strongly charged functional group, previous animal studies have shown that in general the monoquaternary ammonium ions are highly localized in many body tissues. An autoradiographic study of the tissue distribution of several monoquaternary ammonium compounds including TEA in mice was reported by Shindo *et al.* (4). A high accumulation of TEA in the liver and other visceral organs was observed 30 min after a single intraperitoneal injection of [C^{14}]TEA. These data suggest that TEA is either bound extensively to cellular components or transported into tissues against a concentration gradient by specialized carried systems in cell membranes. Our present results from tissue homogenate binding and slice uptake experiments indicate that the high TEA tissue-to-plasma drug concentration gradient is largely due to an active transport system. In addition, the *in vivo* data suggest that transport into the intracellular compartment rather than blood flow may be the limiting factor in the uptake of this cation into tissues. A preliminary mathematical model for TEA featuring active as well

as passive transport processes for the passage of the drug between blood and the tissue mass will be presented here.

MATERIALS AND METHODS

Tetraethylammonium bromide was purchased from Eastman Kodak Co. (Rochester, New York) and used without further purification. [^{14}C]Tetraethylammonium bromide with a specific activity of 2.8 mCi/mM was obtained from New England Nuclear Corporation (Boston). Radiochemical purity (>98%) was checked at 6-month intervals by thin-layer chromatography using the solvent system butanol–ethanol–acetic acid–water (8:2:1:3). Unless specified, the radiolabeled drug was used without the addition of cold carrier. [^{3}H]Dextran (>10 mCi/g) was obtained from Amersham Corporation (Arlington Heights, Illinois).

Adult male Sprague-Dawley strain rats weighing between 250 and 350 g were used. A silastic cannula was chronically implanted into the right heart of each rat via the external jugular vein (5). The animals were allowed to recover from surgery for a period of 24–48 hr. Food was withheld for at least 8 hr prior to an experiment. Water was allowed *ad libitum*. The animals were awake during all the experiments.

Intravenous Bolus Dose Studies

The animals were housed in individual plastic metabolic cages. They were injected through the jugular vein cannula with 2 mg of [^{14}C]TEA dissolved in 0.5 ml of normal saline.

Urinary excretion of [^{14}C]TEA was studied in six rats. Urine was collected at frequent intervals up to 12 hr after intravenous administration. At the end of each interval, voiding of the bladder was induced with ether. The cages were then washed with water and the rinse was added to the urine. In one animal, urine collection was extended to 60 hr to check for the possible delayed appearance of metabolites in urine.

For the plasma and tissue concentration studies, blood samples (100–500 μl) were withdrawn from the venous cannula at designated times after drug administration and collected in heparinized tubes. The blood was centrifuged and plasma separated for radioactivity assay. A total blood volume of no more than 2 ml was taken from any animal in a single experiment. No significant (<5%) drop in the hematocrit was noted. At varying time intervals up to 5 hr the animals were sacrificed by a rapid injection of air into the intravenous cannula. Urine was collected up to the time of sacrifice. The abdomen of the animals was opened immediately. The bladder was irrigated with normal saline and the rinse was pooled with the urine collection.

The visceral organs including the heart, lungs, spleen, liver, kidneys, gonads, and the gut (from esophagus to the rectum) as well as a portion of the skeletal muscle (vastus lateralis) were quickly excised, rinsed well with cold saline, blotted and weighed. To prevent weight loss through evaporation the organs were immediately frozen in an acetone–dry ice bath. The entire skin was stripped from the rat carcass. Sections of the skin from the head, trunk, and tail regions were sampled. The carcass including the diffuse glandular organs (i.e., pancreas and salivary glands), fat, connective tissues, ligaments, and diaphragm were weighed and homogenized in a grinder. A portion of the ground mixture was frozen. All tissues and organs were stored at −20°C pending analysis.

Renal Clearance Studies

Intravenous infusions were performed to measure the renal clearance of TEA in rats at steady state. The animals were restrained in a holder to allow rapid and accurately timed collection of blood and urine. The external jugular vein of the rats was cannulated. A bevel-tip polyethylene tubing (No. 10) was inserted through a 19-gauge thin-wall hypodermic needle into the ventral caudal vein of the rat. An intraveous loading dose of [^{14}C]TEA was administered via the jugular cannula. This was followed immediately by a constant-rate infusion of [^{14}C]TEA into the caudal vein, designed to achieve a steady-state plasma level (C_{ss}) of 0.2 μg/ml. The loading dose (D_1) was calculated from the equation

$$D_1 = V_{ss} \times C_{ss} \tag{1}$$

where V_{ss} is the steady-state apparent volume of distribution. The rate of infusion of TEA (R_0) was calculated according to

$$R_0 = \mathrm{CL}_p \times C_{ss} \tag{2}$$

where CL_p is the plasma clearance of the drug.

Preliminary estimates of V_{ss} and CL_p obtained from the bolus dose experiments were 160 ml and 3.4 ml/min per 100 g body weight (b.w.), respectively. This corresponds to a loading dose of 32 μg/100 g b.w. and an infusion rate of 0.68 μg/min/100 g b.w. for a steady-state level of 0.2 μg/ml. In one animal the loading dose and infusion rate were increased tenfold to achieve a plasma level of about 2 μg/ml.

The initial plasma concentration of [^{14}C]TEA immediately after the administration of the bolus dose usually exceeded the eventual steady-state level. Steady state was reached within 45–90 min after the initiation of the infusion. Plasma radioactivity was monitored at frequent intervals during the equilibration period. Renal clearance measurements did not begin until

two consecutive plasma radioactivity measurements were within 10% of each other. Urine was then collected hourly for 3 hr, and a blood sample was taken at midtimes of the urine collection periods.

At the completion of the renal clearance experiment (about 5–6 hr after the infusion was initiated), the animals were killed and all tissues and organs were sampled in the same manner as described in the previous section. Immediately before the animals were killed, 1 ml of blood was drawn through the jugular vein cannula. The hematocrit of the blood sample was determined. Both the whole blood and plasma [^{14}C]TEA concentration were assayed. The results were used to estimate the partition of TEA between plasma and red blood cells.

In one animal the infusion was carried out for a longer duration, over 12 hr, to check if tissue distribution equilibrium was indeed achieved in the 4–6 hr infusion experiments.

Tissue Homogenate Binding

Rats were stunned by a blow on the head and exsanguinated by severing the jugular vein. The following tissues were immediately removed and placed in ice-cold saline: liver, kidneys, heart, lungs, gut, and carcass. The tissue samples were homogenized and diluted to 10 volumes with 0.25 M sucrose. Known quantities of radioactive tracer and cold TEA were added to the homogenates which were then pipetted into cellophane dialysis bag (4.8 nm pore diameter). Ultrafiltration was carried out in a 37°C thermostatted centrifuge according to the procedure of Schanker and Morrison (6). The ultrafiltrate (about 10% of the initial volume of homogenate) and the homogenate in the dialysis bag were assayed for radioactivity. In control experiments with [^{14}C]TEA spiked *p*H 7.4 phosphate buffer (0.154 M) there was no significant adsorption of drug to the cellophane membrane.

Tissue Slice Uptake Study

Steady-state tissue uptake experiments were performed with the following tissues: kidneys, liver, lungs, heart, and small intestine. Immediately after the animals were killed, the tissues were removed and chilled in ice-cold saline. Except for the intestine, slices of tissues 0.5 mm thick were prepared with the Stadie-Riggs microtome. With liver and kidney, the first two surface slices were discarded. Intestinal rings or slices (from the jejunal section) of 2–3 mm width were obtained by cutting an isolated everted small intestine of the rat. The segments were washed with cold saline and treated in the same manner as the other tissue slices. Two or three slices of tissues weighing between 50 and 250 mg were suspended in 10 ml of Robinson phosphate buffer (*p*H 7.4) containing 0.1% (w/v) of glucose (7). The

medium was spiked with varying amounts of [^{14}C]TEA either with or without the addition of cold drug to yield total drug concentrations between 0.5 and 10 μg/ml. Incubations were carried out in both oxygen (aerobic) and nitrogen (anaerobic) atmospheres according to the procedure described by Dandekar and Kostenbauder (8). When the tissues were incubated under anaerobic condition, carbonylcyamide phenylhydrazone (CCP), a potent uncoupler of oxidative phosphorylation, was added to the incubation medium in a final concentration of 10 μM to ensure total suppression of energy-dependent active transport processes.

The extracellular volume of the various tissue slices was determined with [^{3}H]dextran. Approximately 0.2 μCi of [^{3}H]dextran was added to the incubation mixture. The tissue-to-medium concentration ratio of [^{3}H]dextran gives the volume fraction of extracellular space.

Radiochemical Measurements

Radioactivity of [^{14}C]TEA in plasma or urine was determined by direct liquid scintillation counting (Packard model 3320 liquid scintillation spectrometer). Duplicate 50–250 μl aliquots of plasma or urine were added to glass counting vials containing 10 ml of either dioxane- or toluene-based scintillation fluid (Scintisol, Isolab, Inc., Akron, Ohio). Quenching was corrected by the external standard method. During the early experiments, it was discovered that TEA adsorbs onto glass surfaces (usually a loss of 10–20% in count rate occurred). Therefore, in all subsequent experiments, an excess amount of nonradioactive TEA (10 mg) was added to each scintillation vial. All [^{14}C]TEA solutions were prepared either in plastic containers or in silanized glassware to eliminate the adsorption problem.

Tissue samples from the *in vivo* distribution studies were oxidized to $^{14}CO_2$ (Packard sample oxidizer), and radioactivity was determined by liquid scintillation counting. Except for the gut and gonads, triplicate samples of wet tissues weighing between 250 and 500 mg were combusted. The gut and the gonads were homogenized in 2% (w/v) TEA solution. A 0.5-ml aliquot of the homogenate was assayed in triplicate.

Tissue samples from the slice uptake experiment containing both [^{14}C]TEA and [^{3}H]dextran were also prepared for liquid scientillation counting by the combustion technique. Tritium was oxidized to $^{3}H_2O$ and the radioactivity was determined. The recovery of ^{14}C and ^{3}H radioactivity in the combustion procedure was checked using labeled hexadecane standards. Only results from runs with recovery $>90\%$ were accepted.

Urine collected from the i.v. injection experiments was analyzed for the presence of metabolites by the high-voltage paper electrophoresis method of Conway *et al.* (9). The ^{14}C-radioactivity spots on the electropherogram

were located by a radiochromatogram scanner (Packard model 7201 radiochromatogram scanner). For R_f comparison, an authentic sample of TEA was run alongside the urine sample. Nonradioactive TEA spots were visualized by spraying the chromatograms with Dragendorff reagent.

RESULTS

Single-Dose Intravenous Administration

Cumulative urinary excretion of radioactivity in rats given a 2-mg i.v. bolus dose of [^{14}C]TEA is shown in Fig. 1. The excretion of [^{14}C]TEA

occurred rapidly. Approximately half of the administered radioactivity was recovered in urine in less than 30 min. Within 12 hr more than 96% of the dose was a tage paper electrophc erefore, in rats renal e on. Similar results hav lso showed that biliar 8% of the administer

A ser plasma vs. time follov Vithin 5 hr, plasma TE 25 ng/ml,

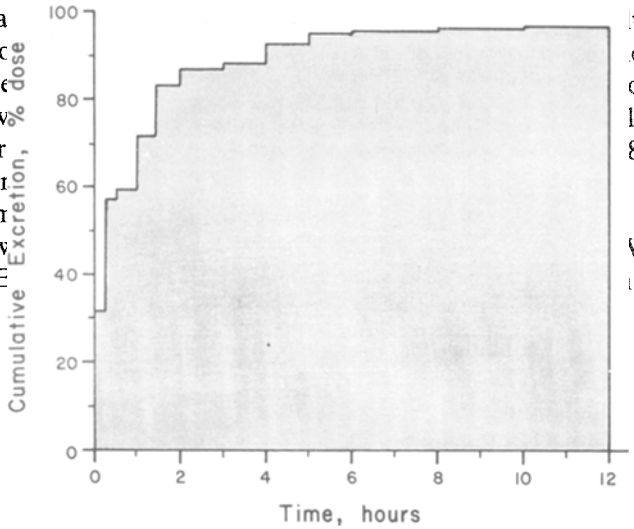

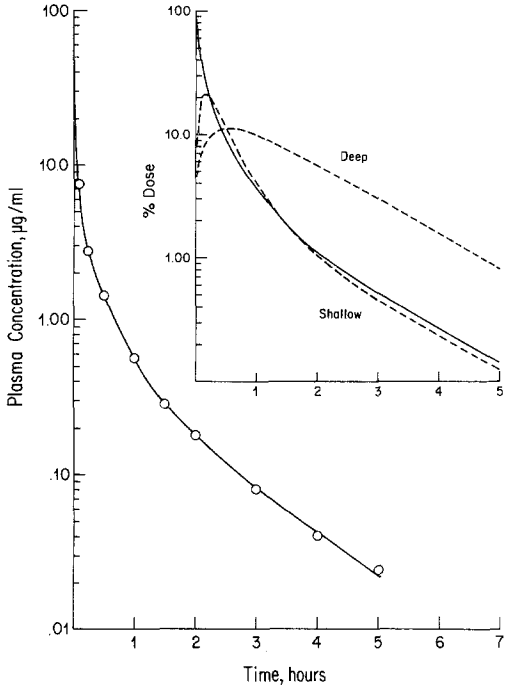

Fig. 2. Plasma concentration–time course of [^{14}C]TEA in the rat following a 2-mg i.v. bolus dose. Each data point represents a mean of four to 17 animals. The continuous curve indicates the nonlinear least-squares regression fit of the plasma concentration data to a classical three compartment model. The inset shows the simulated time course of drug (expressed in % of dose) in the two hypothetical peripheral compartments (– – –) as compared to that in the plasma or central compartment (———).

a level approaching the sensitivity limit of our radioassay. By inspection, the time course of disappearance of TEA from plasma can be resolved into three exponential phases. The plasma concentration data were therefore fitted to the following empirical equation using the NONLIN program of Metzler (11):

$$C = Pe^{-\P t} + Ae^{-\alpha t} + Be^{-\beta t}, \qquad \P > \alpha > \beta \tag{3}$$

Conventional pharmacokinetic treatment of the data would invoke an open three-compartment mammillary model consisting of two tissue compartments, one "shallow" and the other "deep", which are reversibly connected to a central or plasma compartment. In the simplest case, the

elimination of TEA can be assumed to occur from the central compartment. The appropriate transfer and elimination rate constants and the various apparent volume of distribution terms were calculated according to previously established equations (12). Table I lists the parameter estimates. Based on these derived parameters, the time course of drug in the two peripheral tissue compartments was simulated and compared to that in the plasma or central compartment. The net influx of drug into the "shallow" compartment was rapid, reaching a peak within 15 min. The movement of drug into and out of the "deep" compartment was predictably slower. Peak amount was reached between 30 min and 1 hr. The model further predicts that distribution equilibrium should be attained in both tissue compartments within 2 hr after the intravenous injection.

The important parameters to be noted in Table I are the apparent volumes of distribution. The initial distribution space (V_c) is larger than the

Table I. Parameter Estimates[a] of a Three-Compartment Mammillary Model Which Describes the Plasma Level Kinetics of TEA Following a Single Intravenous Bolus Adminstartion to Rats

Parameter	Estimate
P, μg/ml	11.1 ± 0.4[b]
A, μg/ml	3.78 ± 0.24
B, μg/ml	0.559 ± 0.063
¶, hr^{-1}	13.1 ± 1.0
$T_{1/2,¶}$, min	3.17
α, hr^{-1}	2.64 ± 0.16
$T_{1/2,\alpha}$, min	15.2
β, hr^{-1}	0.648 ± 0.033
$T_{1/2,\beta}$, hr	1.07
V_c, ml/100 g b.w.[c]	41.1
V_β, ml/100 g b.w.	312
V_{ss}, ml/100 g b.w.	160
CL_p, ml/min/100 g b.w.	3.38
k_{12}, hr^{-1}[d]	4.10
k_{21}, hr^{-1}	5.46
K_{13}, hr^{-1}	1.07
K_{31}, hr^{-1}	0.835
K_{10}, hr^{-1}	4.92

[a] Obtained by nonlinear least-squares regression analysis of the mean plasma level data (R^2 = 1.00).

[b] Mean ± SD.

[c] Mean body weight of the animals was 314 ± 35 g.

[d] Compartment designation: 1, central; 2, "shallow" peripheral; 3, "deep" peripheral.

plasma volume of the rat, which is 4.04 ml/100 g b.w. (13). In addition, the steady-state volume of distribution (V_{ss}) greatly exceeded the total body water volume for rats, which is 62–70 ml/100 g b.w. (13). This indicates that a substantial portion of the body load of TEA is localized in the tissues.

Renal Clearance

The total body and renal clearances of TEA were measured during continuous intravenous infusion at a steady-state plasma level of approximately 0.2 μg/ml. The results are shown in Table II. The clearance values were expressed on the basis of whole blood concentration, which were calculated using the blood-to-plasma concentration ratio determined in the individual animal. The mean renal clearance for TEA was 3.87 ml/min/100 g b.w., which closely approximates the known effective renal blood flow in rats (i.e., 5.11 ml/min/100 g b.w.) (13). The high renal clearance indicates that secretion occurs in addition to glomerular filtration. Rennick and Moe (14) have shown that in dogs and chickens TEA is rapidly secreted into the proximal tubule via the common base transport system. Since renal excretion is the dominant route of elimination of TEA (the total body clearance was only slightly higher than the renal clearance), the observed steady-state urinary excretion rates of TEA were approximately equal to its infusion rate.

The clearance measurements were repeated in one animal at a tenfold higher steady-state plasma concentration (i.e., 2 μg/ml). The clearance estimates were similar to those obtained at the 0.2 μg/ml level. Renal excretion of TEA appears not to be saturated within this plasma concentration range.

Given the plasma level and urinary excretion data from the i.v. bolus study, the renal clearance of TEA at various time intervals following *acute* drug administration was calculated. The clearance estimates shown in Table III agree with those obtained from our steady-state infusion experiments. It should also be noted that the renal clearance of the drug remained relatively constant over the 5-hr period.

Steady-State Tissue Distribution

In Table IV are listed the steady-state tissue-to-plasma (T/P) concentration ratios obtained in our short-term infusion experiments. The drug was highly concentrated in the visceral organs, *viz.*, kidneys, liver, heart, gut, and lungs, with T/P ratios ranging from 3 to 20. The T/P ratios in the poorly perfused tissues such as gonads, skin, and skeletal muscle were all below 1. In three animals, urine was collected during the entire course of infusion. Since the amount of drug excreted was measured and the infused dose was

Table II. Total Body and Renal Clearance of TEA in the Rat During Steady-State Intravenous Infusion

Rat No.	Weight (g)	Infusion rate (μg/hr)	Plasma concentration (μg/ml)	Blood/ plasma	Excretion rate (μg/hr)	Renal clearance (ml/min/100 g b.w.)		Body clearance (ml/min/100 g b.w.)	
						Plasma	Blood	Plasma	Blood
B-3	356	173	0.275±0.021[a]	0.93	187±4	2.74±0.30	2.95	2.98±0.25	3.20
B-4	298	116	0.194±0.012	0.97	111±4	3.22±0.27	3.32	3.39±0.20	3.49
B-5	304	115	0.156±0.004	0.88	131±3	4.61±0.23	5.24	4.67±0.13	5.30
B-6	319	131	0.191±0.010	0.86	125±17	3.42±0.31	3.98	3.61±0.19	4.20
Mean ± SE ($N = 4$)				0.91±0.02		3.50±0.40	3.87±0.50	3.41±0.46	4.05±0.47
B-12	310	1520	2.08±0.08	0.90	1490±0	3.87±0.13	4.29	3.97±0.13	4.42

[a] Mean ± SE ($N = 3$).

Table III. Renal Clearance of TEA Following a Single 2-mg Intravenous Bolus Dose

Time interval (hr)	AUC[a] (μg-ml^{-1}-hr)	$X_u(t_1-t_2)$[b] (μg)	Cl_R[c] (ml/min/100 g b.w.)
0.0–0.5	2.16	1165	2.87
0.5–2.0	0.823	498	3.22
2.0–5.0	0.220	161	3.89

[a] Area under the plasma concentration–time curve.
[b] Amount excreted in the urine during time interval t_1 to t_2.
[c] Mean animal body weight of 314 ± 8 g.

known, the body load of TEA in these animals at the time of sacrifice can be calculated by difference. This assumes that a negligible amount of drug is lost in the feces. The amount of drug in each tissue, expressed as the percent of body load, is shown in Table V.

Because of a high T/P ratio and its large size, nearly 40% of the body load was localized in the liver. The carcass, which accounts for more than half of the animal weight, contained an additional 20% of the load. Because of its ability to concentrate TEA, 10% of the body burden was confined to the kidneys despite their small size. The balance of the body load, about 30%, was evenly shared by the remaining body tissues. It is interesting to note that an appreciable amount of drug (4–11%) was found in the gut content. Hughes *et al.* (10) have reported a negligible excretion of TEA in the bile. However, recently Turnheim and Lauterbach (15) were able to demonstrate a bidirectional flux of TEA across isolated guinea pig jejunal mucosa. Therefore, the existence of a secretory mechanism in the rat

Table IV. Steady-State Tissue-to-Plasma Concentration Ratio of TEA in the Rat

Tissue	Tissue-to-plasma ratio[a]
Kidneys	19.8 ± 2.0[b]
Liver	19.0 ± 2.0
Heart	9.67 ± 1.2
Gut	3.86 ± 0.19
Lungs	3.39 ± 0.29
Blood	0.91 ± 0.02
Gonads	0.85 ± 0.09
Skin	0.84 ± 0.08
Carcass[c]	0.61 ± 0.03
Muscle	0.38 ± 0.05

[a] At a steady-state plasma concentration of 0.200 ± 0.013 μg/ml.
[b] Mean ± SE ($N = 3$–6).
[c] Including skeletal muscle.

Table V. Tissue Distribution of TEA in the Rat at Steady State[a]

	Percent total body load			
Tissue	B-8	B-9	B-10	Mean
Liver	36.3	39.7	43.4	39.8
Carcass	20.6	21.5	18.2	20.1
Kidneys	11.4	11.9	7.2	10.2
Gut	6.3	7.3	11.3	8.3
Skin	7.4	8.7	8.7	8.3
Gut content	11.0	5.7	4.2	7.0
Blood	2.5	2.8	2.4	2.6
Heart	2.0	1.0	2.5	1.8
Gonads	1.6	0.7	1.3	1.2
Lungs	0.9	0.7	0.8	0.8

[a]Steady-state volume of distribution is estimated to be 156, 244, and 187 ml/100 g b.w. for rats B-8, B-9, and B-10, respectively.

intestinal epithelium may explain the concentration of TEA in gut lumen.

The body load measurement permitted estimation of the actual steady-state volume of distribution (i.e., body load/steady-state plasma concentration). These volume estimates are slightly higher than the predicted value based on the single dose plasma data (Table I).

To assure ourselves that tissue distribution equilibrium was indeed achieved, we have carried out longer-term infusion in one animal lasting 12 hr. The 12-hr infusion data are comparable to those obtained in the earlier group of animals.

Tissue Distribution Kinetics After Intravenous Injection

Figure 3 shows the time course of TEA concentration in various tissues and plasma following a 2-mg bolus injection. The tissue concentration data at each time point represent the mean of two animals. The following observations can be noted:

1. None of the tissues showed a discernible accumulation phase. Tissue concentrations were at maximum within 5–15 min after TEA administration.
2. Only the time course of drug concentration in the liver showed a multiphasic decline which appeared to parallel that of plasma.
3. In contrast, the concentration–time profiles of all other tissues showed a much slower rate of decline.

Hence the T/P ratio of liver showed a modest increase over the first 3 hr and remained relatively constant thereafter, while those of the other tissues

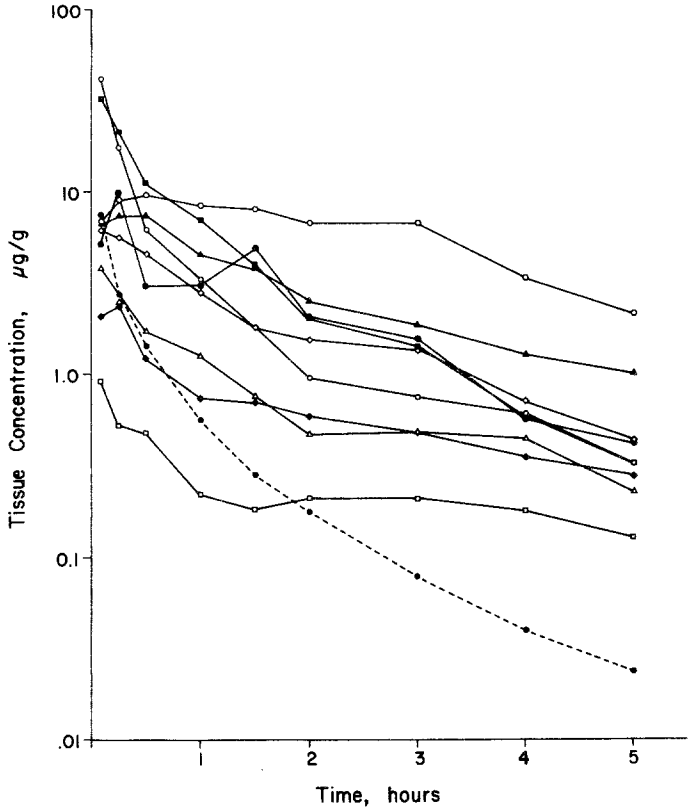

Fig. 3. Time course of [^{14}C]TEA concentration in various tissues and plasma following a 2-mg i.v. bolus injection. The tissue concentration data at each time point represent the mean of two animals. Key: ●--●, plasma; ○, heart; ■, liver; ○, kidney; ▲, gut; ◇, lung; ⬮, carcass (excluding skeletal muscle); △, skin; ◆, gonads; □, muscle.

increased continually with time (Table VI). For example, myocardium-to-plasma ratio rose more than tenfold, from about 7 at 30 min to as much as 89 at 5 hr after drug administration. It is important to note that the T/P ratio at the peak tissue concentration of TEA was much less than the steady-state values as shown in Table IV.

These observations may be explained by different rate of permeation of TEA into the cellular compartment of various tissues and organs. The rate of intratissue distribution of TEA in the liver, in contrast to that in other tissues, appears to be comparable to the organ blood flow. Therefore, distribution equilibrium with the blood pool was reached within 3 hr, which led to a subsequent parallel decline in the time course of concentration in the

Table VI. Time-Dependent Change in Tissue-to-Plasma Ratio of Tetraethylammonium in the Rat Following a 2-mg Intravenous Bolus Dose

	Time (hr)								
Tissue	0.08	0.25	0.5	1.0	1.5	2.0	3.0	4.0	5.0
Kidneys	4.16	6.55	4.26	5.56	6.48	6.69	7.24	12.3	13.2
Liver	3.29	8.10	7.65	10.9	14.5	14.3	13.3	12.4	13.1
Heart	0.69	3.43	6.67	13.8	29.3	47.9	63.3	71.1	88.8
Gut	0.67	2.80	5.05	7.12	13.9	18.4	17.6	27.1	41.1
Lungs	0.61	2.13	3.15	4.47	6.51	10.8	13.1	14.9	18.1
Gonads	0.21	0.92	0.84	1.21	2.57	4.00	4.65	7.40	11.4
Skin	0.38	0.96	1.18	2.07	2.79	3.24	4.69	8.71	9.20
Carcass[a]	0.53	3.88	2.10	4.64	18.7	13.4	16.2	12.3	17.5
Muscle	0.09	0.20	0.32	0.37	0.66	1.41	2.00	3.69	5.18

[a] Excluding muscle.

liver organ with that in plasma. With the other organs and tissues, a continual uptake of TEA into the cellular compartment may be occurring while the overall tissue concentration was falling. This would explain the much slower rate of decline.

In light of the pronounced time-dependent variation in T/P ratios, the distribution of TEA body load at various times following the bolus administration were examined. It should be noted that near complete recovery of the administered dose of radioactivity (81–97%) from blood, tissues, and urine was achieved at each sample time. The data presented in Table VII

Table VII. Amount of TEA in Various Rat Tissues Expressed as Percent Body Load Following a 2-mg Intravenous Bolus Dose

	Time (hr)								
Tissue	0.08	0.25	0.5	1.0	1.5	2.0	3.0	4.0	5.0
Kidneys	10.1	5.36	3.37	2.77	1.98	1.35	1.01	1.27	1.00
Liver	28.5	30.0	26.1	23.5	17.8	11.0	8.10	5.57	3.85
Heart	0.62	1.14	2.10	2.64	3.37	3.41	3.64	3.04	2.34
Gut	5.46	9.61	14.7	12.8	15.6	15.6	12.4	11.3	11.4
Gut content	3.48	6.14	8.60	12.2	18.7	23.7	30.7	29.6	35.1
Lungs	0.70	0.88	1.20	1.14	1.38	1.44	1.21	0.76	0.67
Blood	10.5	3.75	3.43	2.16	1.14	0.81	0.71	0.38	0.33
Gonads	1.07	1.48	1.53	1.23	1.50	1.71	1.82	1.52	1.67
Skin	16.2	15.0	15.0	19.4	13.2	9.69	12.6	15.4	12.0
Carcass[a]	12.5	18.7	12.1	14.0	16.7	18.7	12.8	12.9	13.0
Muscle	10.3	8.05	11.5	8.15	8.47	12.4	14.6	18.1	18.4

[a] Excluding muscle.

show that while a relatively constant portion, about 30%, of the body load is found in the poorly perfused tissues (i.e., skin, skeletal muscle, and carcass), there is a notable shift in the distribution pattern among the viscera organs over the 5-hr period. There appears to be a continual concentration of TEA in the gut tissue and in the gut lumen content with time. The accumulation of TEA in the gut lumen is especially noticeable. In contrast, there occurs a steady decline in the relative body load of TEA in both the kidneys and the liver. At 5 min after injection, about 40% of the body load is localized in the liver and kidneys compared to less than 10% in the tissue and lumen of the gut. A reversed situation is seen by 5 hr after drug administration. Clearly, the secretion of TEA into the gastrointestinal tract is an important factor in the kinetics of drug elimination from the body at later times.

Localization of a drug in body tissues can be attributed to several mechanisms, including (1) reversible binding of the drug to proteins or other tissues constituents, (2) "solubilization" of a lipophilic drug in the lipoid component of cellular structures, (3) the existence of a *p*H difference between the intra- and extra-cellular fluids, and (4) the existence of a transport system for the drug across cell membrane. Since TEA is a charged species in physiological fluids, mechanisms 2 and 3 can reasonably be ruled out. *In vitro* experiments were conducted to ascertain if binding and/or transport may be responsible for maintaining the high T/P ratios observed in the visceral tissues.

Tissue Homogenate Binding

The ability of various rat tissues to bind TEA was determined with a 10% (w/v) homogenate of tissue in 0.25 M sucrose using an ultrafiltration procedure. The results are presented in Table VIII. Tetraethylammonium exhibited negligible binding affinity toward all of the tissue homogenates

Table VIII. Rat Tissue Homogenate Binding

Tissue	Homogenate concentration (μg/ml)	Ultrafiltrate concentration (μg/ml)
Kidneys	5.27	5.46
Liver	5.18	5.27
Heart	11.0	11.0
Gut	2.74	2.78
Lungs	2.64	2.67
Gonads	0.97	0.99
Carcass[a]	2.40	2.60
Muscle	0.31	0.32

[a] Including skeletal muscle.

tested. Either the binding capacity of the tissues is diminished after homogenizing the tissues, or there occurs in the intact tissue a process other than binding that accounts for the high degree of localization of the drug.

Uptake by Tissue Slices

Slice uptake experiments were performed on those tissues which have *in vivo* steady-state T/P ratios exceeding 1. Drug concentration in the incubation medium was varied from about 0.1 to 10 μg/ml. This concentration range is consistent with the *in vivo* circulating plasma concentrations observed during the i.v. bolus dose study. The uptake of TEA by the tissue slices (see Fig. 4a,b) was compared to that of a nonabsorbable, extracellular volume marker, i.e., [^{3}H]dextran. In all five tissues, TEA accumulated to a greater extent than dextran, indicating that uptake into cells occurred. Furthermore, an enhanced uptake into slices was observed when the incubation was carried out under an oxygen atmosphere as compared to a nitrogen atmosphere plus the presence of the metabolic poison, CCP.

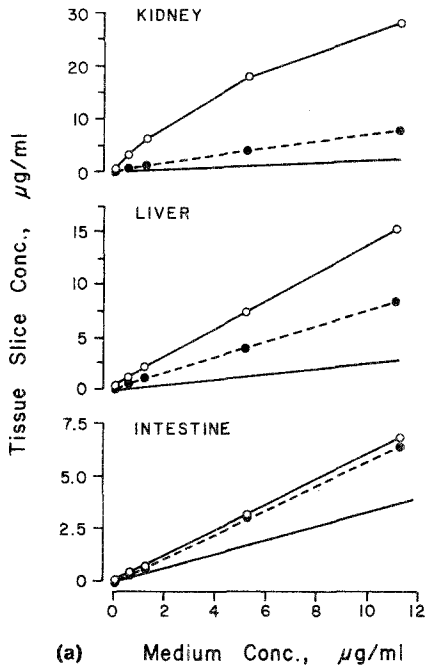

Fig. 4a. Steady-state uptake of [^{14}C]TEA by incubated rat tissue slices. Key: ○——○, under aerobic conditions; ●– – –●, under anerobic condition and in the presence of a metabolic inhibitor (CCP); ———, uptake of an extracellular volume marker ([^{3}H]dextran).

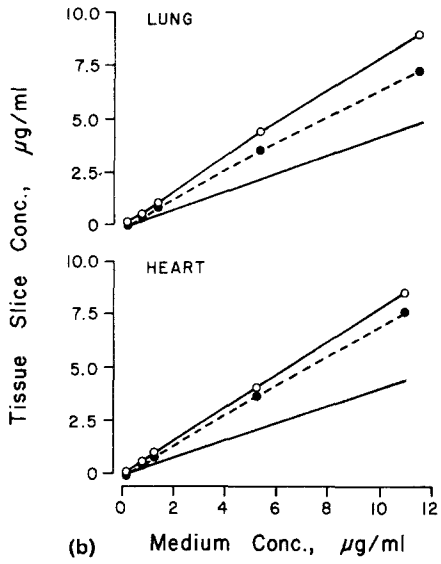

Fig. 4b. Steady-state uptake of [^{14}C]TEA by incubated rat tissue slices. See (a) for details.

Transport of TEA into rat tissues is therefore mediated by both a passive and an energy-dependent or active process.

Active uptake was most prominent in kidney and liver slices. Steady-state uptake of TEA into kidney slices appears to be saturable over the chosen range of medium concentration whereas linear uptake was observed in other tissues. It is possible that capacity-limited uptake can also be demonstrated in other tissues if the medium concentration is increased beyond 10 μg/ml. Saturable active uptake of TEA by renal cortical slices from rats (8), mouse (16), and dogs (17) has been demonstrated previously.

The uptake of TEA from tissue slices from the intestine, lungs, and heart appears to occur mainly via a passive process. The exact nature of this passive component of uptake is presently not known. Simple passive diffusion due to an electrochemical gradient across the cell membranes and/or facilitated diffusion mediated by a specialized carrier may occur. In addition to diffusion, uptake under anaerobic condition can be attributed to adsorption of drug onto intact cell surface, even though significant binding to tissue homogenates could not be demonstrated.

It should be noted that even though the uptake of TEA into intestinal rings was consistently higher in the presence of oxygen, the increase over that achieved under the inert atmosphere was minimal and statistically insignificant. In retrospect, this lack of difference in TEA uptake under the two different conditions may not be surprising. Active transport is most likely to take place in the mucosal epithelium. However, cross-sectional

slices of the intestine include both the epithelium and the underlying muscularis. Hence the results of our uptake study may have been more revealing if isolated rat mucosa was used instead of gross sections of the intestine. Turnheim and Lauterbach (15) have, in fact, demonstrated saturable active transport of TEA in the isolated jejunal mucosa of guinea pig.

Although the tissue slice experiments revealed the mechanisms by which TEA enters tissues, the tissue-to-medium (T/M) concentration ratios of the slices were far below the T/P ratios observed *in vivo*. For example, the maximum *in vitro* T/M ratio for the kidney was about 7 as compared to an *in vivo* steady-state T/P ratio of about 20. Nonetheless, there appears to be a reasonably good rank-order correlation between the *in vitro* T/M and the *in vivo* T/P ratios. It is also important to note that only net steady-state uptake was measured in our tissue slice experiments. These data alone do not indicate whether active transport is bidirectional or only in the direction of medium to slice.

Development of the Model

A schematic of the compartmental model used to fit the experimental data is shown in Fig. 5. All pertinent tissues for which drug concentrations are known have been included. The various tissue regions are interconnected by the blood circulatory network. The organ flow rates and volumes of the various tissues were taken from published physiological values (18,19) and adjusted to reflect the size of the animals studied. Each of the tissue compartments can be subdivided into the three following fluid compartments: (1) the capillary blood volume, (2) the interstitial water, and (3) the

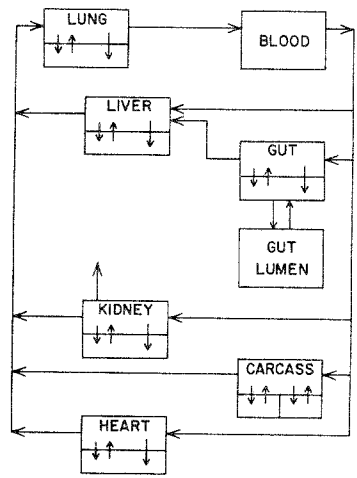

Fig. 5. Compartmental flow diagram for TEA in the rat.

intracellular space. Exchange of drug between the capillary blood and interstitial water is generally considered to be quite rapid. These fluids were therefore combined into one equilibrium space, i.e., the extracellular fluid. As a further simplification of the model, the cell membrane was considered to be very permeable to the drug, in which case the concentration of a drug in the effluent (venous) blood from a tissue region may be assumed to be in equilibrium with that in the tissue. In effect, the uptake of such a drug into tissue is rate-limited by blood flow. A typical mass-balance rate equation of a drug in a noneliminating tissue under blood-flow-rate-limiting condition is written as

$$V_i' \, dC_i'/dt = Q_i(C_B - C_i'/R_i) \tag{4}$$

The nomenclature for this equation and others are defined in Appendix I. It should be noted that C_i' is the experimentally measured concentration of drug in wet tissue samples which includes the residual or equilibrium blood. The tissue-to-blood *distribution ratio*, R_i, under the flow-limiting conditions represent linear binding or nonsymmetrical transport of the drug in the tissue. Since at steady-state equilibrium

$$(dC_i'/dt)_{ss} = 0$$

rearrangement of equation 4 yields

$$(C_B)_{ss} = (C_i')_{ss}/R_i$$

or

$$R_i = (C_i')_{ss}/(C_B)_{ss} \tag{5}$$

When the estimates of R_i for TEA in rats were taken from the steady-state infusion data given in Table IV and when the flow-limiting model composed of a set of equations similar to equation 4 were solved numerically on a digital computer, a satisfactory representation of the data could not be achieved. Essentially, the flow model predicted that distribution equilibrium should be achieved (i.e., a constant T/P ratio was reached) within minutes after drug administration. This is in striking contrast to the observed data, which showed continual uptake of TEA into tissues as indicated by increasing T/P ratios over the 5-hr study period. In retrospect, the prediction of rapid equilibration of drug between tissues and plasma in the rat by the flow model is to be expected. Under the flow-limited assumption, a slow distribution (on a time scale of hours) can occur only when the drug has a high affinity for a poorly perfused or inaccessible tissue such as adipose tissue or bone marrow or when there is an appreciable degree of enterohepatic circulation. Neither of these processes is involved in the disposition of TEA in the rat. Furthermore, Coleman *et al.* (20) have

pointed out that small animals, and rodents in particular, show a whole-body blood flow per unit weight, including blood flow to skeletal muscle, that is considerably greater than comparable flows in large mammals and man. The increased blood flow per unit weight facilitates distribution to the large, poorly perfused tissue regions.

Since the flow-limiting model did not adequately represent the experimental data, a model which includes diffusive transport of drug into the tissues is considered next. A differential mass balance for the equilibrium blood pool and a typical non-eliminating tissue are shown in the following:

Equilibrium blood:

$$V_{iB}\, dC_{iB}/dt = Q_i(C_B - C_{iB}) + K_i(C_{iT}/\psi_i - C_{iB}) \tag{7}$$

Tissue

$$V_{iT} dC_{iT}/dt = K_i(C_{iB} - C_{iT}/\psi_i) \tag{8}$$

The permeability coefficient is given the symbol K_i. Note that C_{iT} now denotes the actual tissue concentration of drug. The term ψ_i is the equilibrium tissue-to-blood distribution coefficient, since at steady state equations 7 and 8 reduce to

$$\psi_i = (C_{iT})_{ss}/(C_{iB})_{ss} = (C_{iT})_{ss}/(C_B)_{ss} \tag{9}$$

In turn, ψ_i can be related to the experimentally determined distribution ratio R_i by the following equation:

$$\psi_i = R_i(V_{iB} + V_{iT})/V_{iT} - V_{iB}/V_{iT} \tag{10}$$

Here ψ_i represents only linear binding of drug in tissue:

$$\psi_i = \Phi_i/\Phi_B = \text{unbound fraction in blood/unbound fraction in tissue} \tag{11}$$

Estimates of the diffusional permeability (K_i) were made and the differential equation set was solved. Again, the model failed to provide an adequate representation of the data. The model simulations underestimated the tissue concentrations at early times, whereas at late times the predicted tissue concentrations exceeded the observed data.

The reason for the poor results with the linear diffusion model are best seen by examining both experimental (direct) and theoretical (indirect) evidence for active transport of the drug into (and out of) the tissues. Indirect pharmacokinetic evidence for active transport is illustrated by considering the simulations presented in Fig. 6. In the first case, the time course of uptake of a drug into a well-perfused (but typical) rat tissue with a high permeability (K_i) and a small distribution coefficient (ψ_i) is presented with

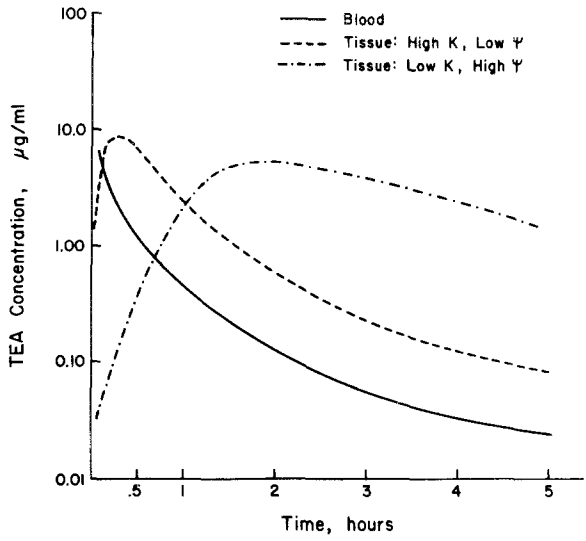

Fig. 6. Comparison of the time course of drug uptake into a well-perfused hypothetical rat tissue with a high permeability (K) and a small distribution coefficient (ψ) to that with a low permeability and a large distribution coefficient.

the blood data. A high peak tissue concentration is reached very shortly after drug administration. The tissue-to-blood (T/B) ratio remains relatively constant over the course of the simulation. Figure 6 also shows the alternate case of a hypothetical tissue having a low permeability and a large distribution ratio. Peak concentration is reached at relatively late times after administration of drug. After peak tissue concentration is reached, the T/B ratio continues to increase over time. It should be noted that in both simulations the T/B ratio at the time of peak tissue concentration is equal to that at steady state since the tissue and blood pool are in instantaneous equilibrium. The actual TEA tissue data, as shown in Fig. 3, show that peak concentrations were reached very quickly after the intravenous injection, somewhere on the order of 5–30 min. Thus one would expect the first model (i.e., high K_i and small ψ_i) to be appropriate for TEA uptake into the well-perfused tissues. However, as was pointed out earlier (Table VI) the T/P ratio for most tissues continually increased over the course of the entire experiment, which conforms rather to the behavior as predicted according to the alternate model. As such, no combination of K_i and ψ_i adequately explained the TEA uptake data. This indirect pharmacokinetic evidence suggests that other uptake mechanisms in addition to simple diffusion must be operating in the movement of TEA into intracellular sites. The tissue slice uptake data definitely indicate the involvement of an active transport

mechanism. It is also intuitive that an active transport process would allow continued concentration of drug into tissues at late times while at the same time diffusion would lead to the early peak times found experimentally to occur for the well-perfused tissues.

Figure 7 is a schematic representation of a tissue region which includes both active and passive transport of a drug. The mass-balance for the tissue equilibrium blood is shown in equation 12:

$$V_{iB}\, dC_{iB}/dt = Q_i(C_B - C_{iB}) + K_i(C_{iT}/\psi_i - C_{iB}) - V_{m_i}C_{iB}/(K_{m_i} + C_{iB}) \tag{12}$$

Similarly, for the tissue pool,

$$V_{iT}dC_{iT}/dt = K_i(C_{iB} - C_{iT}/\psi_i) + V_{m_i}C_{iB}/(K_{m_i} + C_{iB}) \tag{13}$$

As a first approximation, it was assumed that active transport of TEA is unidirectional, i.e., only transport into the cellular compartment is allowed. This restriction was imposed due to practical considerations, since, with the added degree of freedom, approximate estimates of the various transport and binding parameters cannot be obtained with the available data.

Active transport of TEA into the tissue pool was assumed to occur in all of the well-perfused tissues, *viz.*, the kidneys, liver, heart, lungs, and gut. We also assumed that the equilibration of TEA between the erythrocytes and plasma water occurs instantaneously. Hence blood and plasma concentrations can be interconverted using the average blood-to-plasma ratio of 0.9 (Table II). Also, since intracellular binding of TEA cannot be demonstrated in any of the well-perfused tissues, ψ_i was set equal to unity.

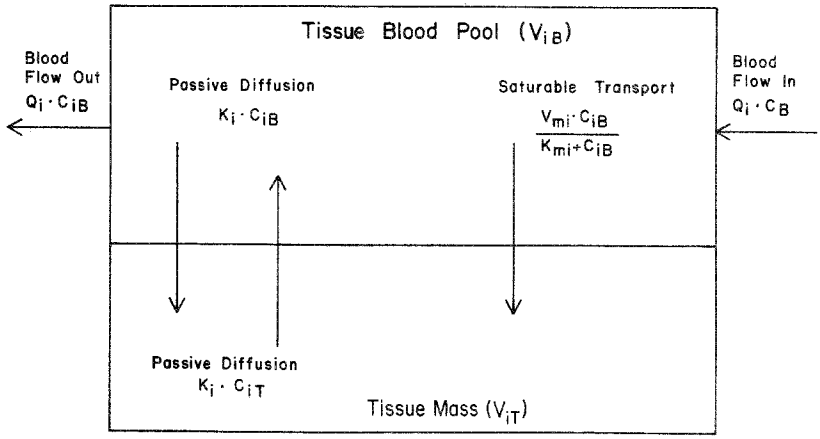

Fig. 7. Schematic representation of a tissue region which includes both active and passive transport of a drug.

The gut lumen is considered as a separate compartment because of the presence of significant quantities of TEA. Linear transport of drug across the intestinal mucosa was found to adequately describe the accumulation of TEA in the lumen. It was also necessary to assume that TEA is bound to some constituents of gut fluid. This assumption is based on the experimental observation of Levine *et al.* (21), which indicated that monoquaternary ammonium ions can form nonabsorbable complexes with constituents of intestinal mucin, most likely polysaccharides. Over the course of the experiment, clearance of TEA from the gut lumen via fecal excretion was assumed to be negligible.

The data presented in Table III indicate a relatively constant clearance of TEA from blood by the kidneys (i.e., between 3 and 4 ml/min/100 g b.w.) during the washout period. The glomerular filtration rate (GFR) for rats is approximately 1 ml/min/100 g b.w. The difference between TEA renal clearance and the GFR respresents the contribution of the proximal tubular secretion process (assuming reabsorption of TEA does not occur in the distal renal tubule). If a linear secretion term is used for the additional 2–3 ml/min/100 g b.w. of clearance, it is found that urinary excretion of TEA in the early time period (i.e., 0–10 min) was overpredicted. A saturable tubular secretion of TEA was thus assumed. The parameters for this secretion term were estimated from early time points on the excretion curve and adjusted to give clearance of 12 ml/min for times greater than 30 min.

It was decided at the outset that the gonads, skeletal muscle, skin, and the "carcass" (i.e., all those tissues not specifically separated out) will be lumped into a single tissue compartment which will be designated, for lack of a better term, as the carcass from here on. The reasons for pooling these tissues are several. First, they are anatomically heterogeneous tissues, and, because of sampling difficulties, a detailed breakdown was not attempted. Second, they are all poorly perfused tissues with similar TEA washout kinetics.

The peak concentrations for these poorly perfused tissues are reached within the first half hour after drug administration if not earlier. This indicates a relatively rapid uptake of TEA into these tissues. The ratio between peak tissue concentration and the plasma concentration at the corresponding time was much lower than that found in the well-perfused tissues. Also, the steady-state R_i ratio was less than 1 for all of the tissues in this lumped compartment. Thus the carcass compartment appeared to exhibit a very low distribution coefficient ψ_i with rapid passive transport (i.e., high K_i). This assumption fits well for the first 2 hr. However, the high K_i led to a much faster terminal rate of decline than was actually observed. One explanation may be that among the carcass tissues (even in the skeletal muscle alone) there are at least two regions which exhibit different

permeability toward TEA. We were not able to model these data as a single homogeneous tissue even when an active transport process was incorporated. Thus the carcass tissues are represented by two tissue compartments each in exchange with a common equilibrium blood pool. The two compartments have different distribution coefficient and permeability. While the apparent volumes of these two subcompartments are chosen arbitrarily, the volume of each compartment is set such that most of the drug in the carcass is in the rapidly equilibrating tissue at short times and most of the drug at long times is in the slowly equilibrating tissue, with the constraint that the total load of the two compartments equals the observed carcass data. Hence the concentration achieved in two tissues separately has no meaning, but the mass of the drug divided by the total volume of these two tissues should equal to the concentration of the drug found in the overall carcass. Several possible arrangements for these two tissues are possible. Two tissues in series or two tissues in parallel give approximately the same results. It has not been possible to experimentally measure which of these models is to be chosen. A parallel distribution model as shown in Fig. 5 is chosen. This decision is arbitrary, and as further experimental data are developed the model can be modified to include the proper physiologically representative compartments for the poorly perfused tissues.

Mass balances were written for each of the tissues and blood. The complete set of differential equation is given in Appendix II. The differential equations were solved numerically by a modified Hammings predictor-corrector integration scheme (22). Methods for obtaining initial estimates of permeability and active transport parameters are described in Appendix III. The parameter estimates were adjusted through repeated simulations until a best visual fit of the observed data was achieved.

The final estimates of the various parameters of the model are listed in Table IX. The results of the simulations are shown in Fig. 8–14. There was a reasonably good fit of the model simulation to the observed tissue and blood data.

DISCUSSION

The classical pharmacokinetic models derived solely on the basis of blood/plasma and excreta data are now widely utilized in disposition studies of drugs in animals and man. Unfortunately, these types of empirical models, by their very nature, cannot be expected to accurately predict events occurring at extravascular sites. This is particularly so when the uptake of drug into tissue is slow. One then observes the typical multiphasic decline of

Table IX. Model Parameters

Tissue	V_i (ml)	Q_i (ml/min)	K_{m_i} (μg/ml)	Vm_i (μg/min)	K_i (ml/min)	Others
Blood	17.0	63.0	—	—	—	—
Liver blood	1.97	5.0	3.0	75.0	2.0	—
Liver	12.1	—	—	—	—	—
Kidney blood	1.1	15.0	1.0	60.0	0.8	$k_{GF} = 10$ ml/min $K_{mTS} = 0.33$ μg/ml $V_{mTS} = 17$ μg/min
Kidney	2.2	—	—	—	—	—
Gut blood	0.655	16.0	2.0	9.0	0.3	—
Gut	12.3	—	—	—	0.35	$\psi_{GL} = 3.0$
Gut lumen	5.0	—	—	—	—	—
Lung blood	0.9	63.0	0.3	0.5	0.05	—
Lung	0.91	—	—	—	—	—
Heart blood	0.22	3.0	0.065	0.32	0.03	—
Heart	0.88	—	—	—	—	—
Carcass blood	7.5	24.0	—	—	—	—
Carcass, rapid	200.0	—	—	—	400	$\psi_{CrR} = 0.67$
Carcass, slow	30.0	—	—	—	0.5	$\psi_{CrS} = 0.85$

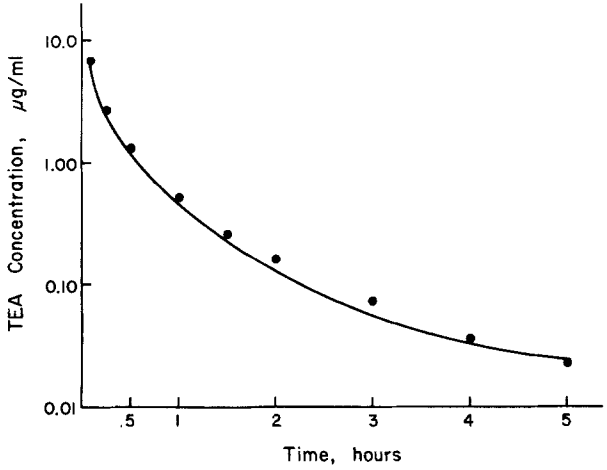

Fig. 8. Predicted (continuous line) vs. observed (points) time course of [^{14}C]TEA concentration in rat blood following a 2-mg bolus i.v. injection.

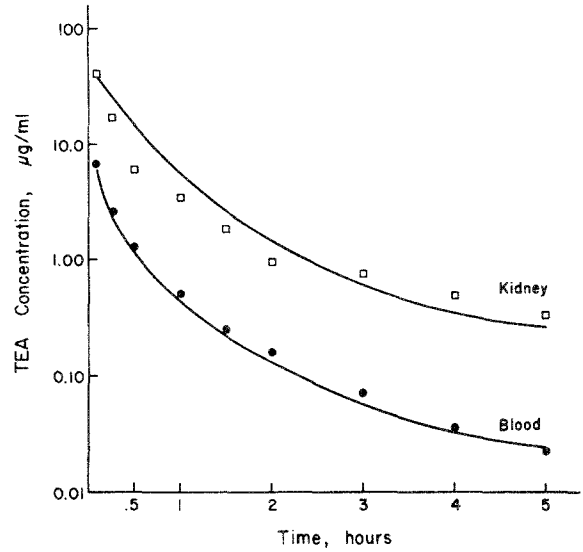

Fig. 9. Predicted vs. observed time course of [^{14}C]TEA concentration in the kidney and blood of the rat following a 2-mg bolus i.v. injection.

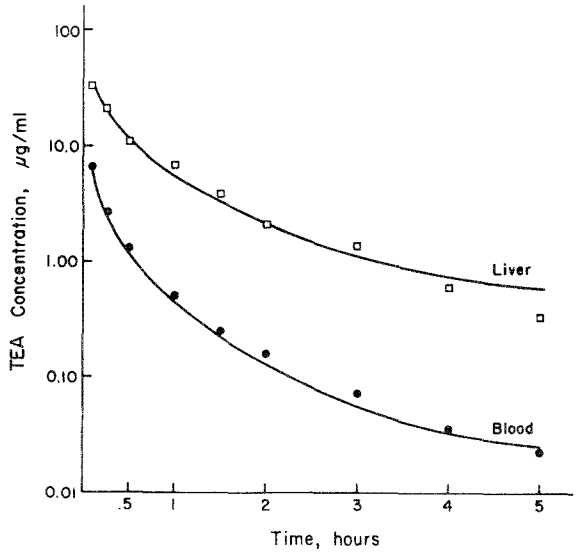

Fig. 10. predicted vs. observed time course of [^{14}C]TEA concentration in liver and blood of the rat following a 2-mg bolus i.v. injection.

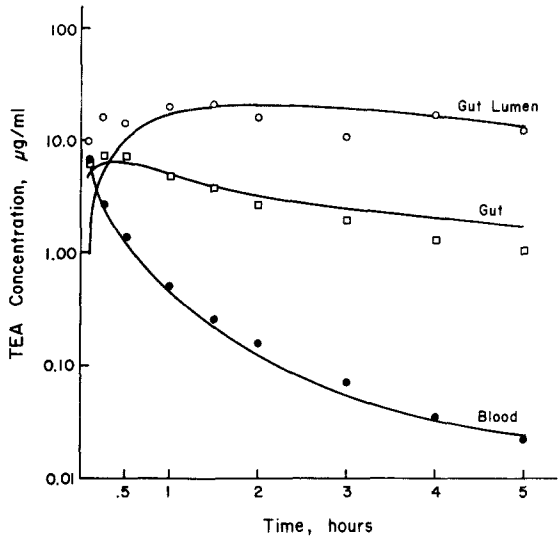

Fig. 11. Predicted vs. observed time course of [^{14}C]TEA concentration in the gut, gut lumen, and blood of the rat following a 2-mg bolus i.v. injection.

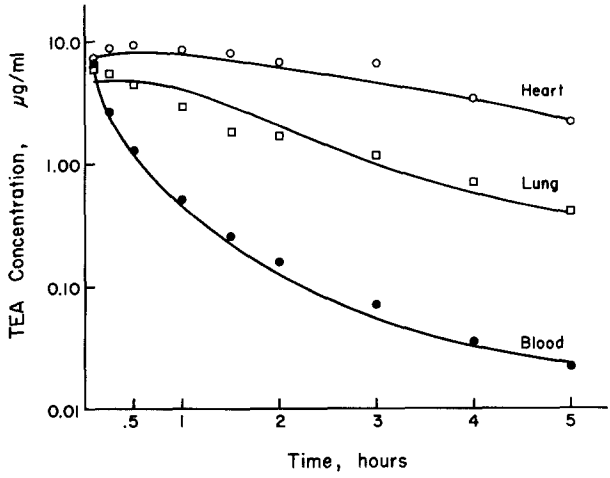

Fig. 12. Predicted vs. observed time course of [^{14}C]TEA concentration in the heart, lung, and blood of the rat following a 2-mg bolus i.v. injection.

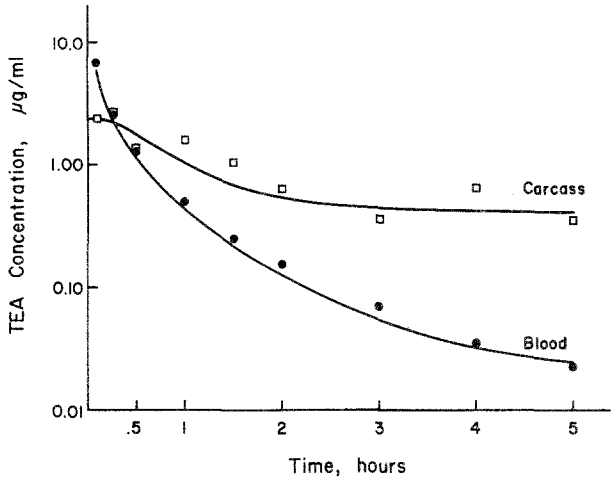

Fig. 13. Predicted vs. observed time course of [^{14}C]TEA concentration in the carcass (including skeletal muscle and gonads) and blood of the rat following a 2-mg bolus i.v. injection.

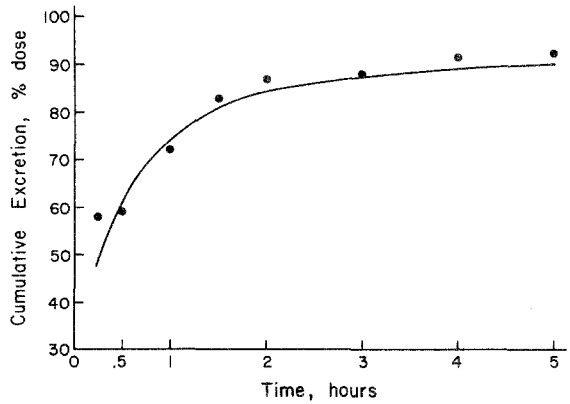

Fig. 14. Predicted vs. observed cumulative urinary excretion of [^{14}C]TEA in the rat.

plasma drug concentration with time on a semilogarithmic plot, which most often leads to the proposal of a multicompartment mammillary-type model (23). The hypothetical peripheral compartments in these models do not represent actual tissues or organs and may at best be regarded as being "hybrids of several more complex physiologic units" (24). In some rare instances, the predicted drug concentration in these peripheral compartments may parallel the actual concentration of drug in tissues (25). The present tissue distribution study of TEA in rats further emphasizes the limitation of classical pharmacokinetic models in dealing with the uptake of drug into tissues and organs. Specifically, it shows that when tissue uptake involves saturable transport processes, the time course of drug concentration in blood or plasma simply does not reflect or in any way provide an indication of the dynamics of drug accumulation and washout in tissues. As can be seen by comparing Figs. 2 and 3, there is little correspondence between the classical linear compartmental model simulation and the actual time course of drug concentration in the various tissues. While the classical model based on plasma data suggests that distribution equilibrium is essentially complete by 2–3 hr after TEA administration, the actual T/P ratios rise continually over the entire study period, indicating that distribution equilibrium would not be fully established in less than 5 hr. Presumably a constant T/P ratio will be attained only when TEA concentration in the perfusing blood has fallen to a level well below the K_m of the membrane transport carrier. The above discussion points to a definite need to develop more realistic and unavoidably more sophisticated pharmacokinetic models if the tissue distribution kinetics of drugs are to be fully appreciated.

The *in vitro* rat tissue uptake data of TEA warrant some comments. Initially, the tissue slice incubation studies were performed with the expectation that an *in vitro* means of estimating the transport and permeability parameter would be possible. It was rather disappointing (but perhaps not surprising) to find that the slices were not able to concentrate TEA to the degree observed *in vivo*. This lack of an agreement between *in vitro* T/M and *in vivo* T/P ratio can largely be attributed to the methodological problems in using slices as an experimental model to studying cellular drug transport. Although the incubated slice technique offers the advantages of being techniqally simple and readily applied to a variety of tissues, it is generally recognized that the metabolic performance of the incubated slices is far removed from that of the organ in an intact animal (26,27). A rapid loss of cellular viability inevitably occurs during the incubation procedure. Maintaining the metabolic integrity of an *in vitro* isolated tissue preparation is essential when active transport functions are being studied. A deterioration in the active transport function would explain the decreased ability of the incubated tissue slices to accumulate TEA.

There is an additional complication in interpreting *in vitro* slice uptake data. The tissue slice has no capillary circulation, and all exchanges between the tissue and the suspending medium must occur by diffusion through distances up to half the thickness of the slice (i.e., at least 0.25 mm). Kinetic measurements with extracellular markers show that a lag time as long as 20 min may be required before the extracellular space equilibrates with the bathing medium. Thron (28) has recently provided an excellent discussion of the complications introduced by this diffusion delay in the kinetic interpretation of uptake and washout data of a substance in an isolated tissue preparation. At present, the most valid experimental approach to studying tissue uptake appears to be the isolated organ perfusion technique. The perfusion technique, however, has the disadvantages of being technically demanding and time consuming. In recent years, methods for preparing isolated cells from various mammalian organs have been reported. In general, the metabolic activity of these isolated cell preparations can be maintained for a sufficient length of time. In addition, since the individual cells are in full contact with the suspending medium, the complication of a diffusion lag is eliminated. Perhaps in the future when these isolation techniques become more commonly available, they may eventually be employed to provide reliable *in vitro* estimates of drug transport and permeability parameters.

It appears then that until such time when reliable *in vitro* means of quantitating drug transport are available, a truly *a priori* model for the tissue distribution of drugs is not feasible. In view of the poor *in vitro–in vivo* correlation of TEA tissue uptake data, we adopted a semi-empirical curve-fitting approach in estimating the necessary tissue uptake parameters.

Although our present model was able to provide a good prediction of the intravenous bolus dose data over the 5-hr period, there are still a number of deficiencies. First, we need to identify the slow and rapid uptake tissues that presently compose the carcass compartment. It would be desirable to measure the concentrations of drug in the smaller suborgans (e.g., skeleton and salivary glands) that were not examined in this study. Second, the assumption of a unidirectional (i.e., from extracellular space to inside the cells) active transport system is probably not realistic. The *in vitro* tissue uptake studies on the kidneys and intestinal mucosa, reported by Holm (16) and Turnheim *et al.* (15), respectively, indicate that active transport of TEA occurs in both directions. In fact, preliminary simulation of steady-state infusion with the model shows that, in general, the predicted tissue concentration at a plasma concentration of 0.2 μg/ml is higher than that observed. In order to fully characterize the kinetics of the active transport mechanism, further studies at other doses or concentrations will be required.

APPENDIX I: NOMENCLATURE

General

V, Volume of tissue (excluding equilibrium blood), ml
V', Volume of tissue (including equilibrium blood), ml
Q, Flow rate of blood through tissue, ml/min
C, Tissue concentration (excluding equilibrium blood), μg/ml
C', Total tissue concentration (including equilibrium blood), μg/ml
K, Permeability, ml/min
V_m, Maximum transport velocity, μg/min
K_m, Half-saturation concentration for transport, μg/ml
R, Distribution ratio
ψ, Distribution coefficient
Φ, Reciprocal of unbound fraction
k, Renal clearance, ml/min
$\dot{V}$, Urine flow rate, ml/min
$\delta(t)$, Dose input function

Subscripts

B, Blood pool
Li, Liver compartment
LiB, Liver equilibrium blood
LiT, Liver tissue
K, Kidney compartment
KB, Kidney equilibrium blood
KT, kidney tissue
G, Gut compartment
GB, Gut equilibrium blood
GT, Gut tissue
GL, Gut lumen
Lu, Lung compartment
LuB, Lung equilibrium blood
LuT, Lung tissue
H, Heart compartment
HB, Heart equilibrium blood
HT, Heart tissue
Cr, Carcass compartment
CrB, Carcass equilibrium blood
CrR, Rapidly equilibrating carcass tissue
CrS, Slowly equilibrating carcass tissue
GF, Glomerular filtration
TS, Renal tubular secretion
U, Urine

APPENDIX II: MODEL EQUATIONS

Blood:

$$V_B\, dC_B/dt = Q_B(C_{LuB} - C_B) + \text{dose} \times \delta(t) \tag{14}$$

Liver:

$$V_{LiB}\, dC_{LiB}/dt = Q_{Li}(C_B - C_{LiB}) + Q_G(C_{GB} - C_{LiB}) + K_{Li}(C_{LiT} - C_{LiB}) - V_{m_{Li}} C_{LiB}/(Km_{Li} + C_{LiB}) \tag{15}$$

$$V_{LiT}\, dC_{LiT}/dt = K_{Li}(C_{LiB} - C_{LiT}) + V_{m_{Li}} C_{LiB}/(Km_{Li} + C_{LiB}) \tag{16}$$

Kidney:

$$V_{KB}\, dC_{KB}/dt = Q_K(C_B - C_{KB}) + K_K(C_{KT} - C_{KB}) - V_{m_K} C_{KB}/(K_{m_K} + C_{KB}) - - k_{GF} C_{KB} - V_{m_{TS}} C_{KB}/(K_{m_{TS}} + C_{KB}) \tag{17}$$

$$V_{KT}\, dC_{KT}/dt = K_K(C_{KB} - C_{KT}) + V_{m_K} C_{KB}/(K_{m_K} + C_{KB}) \tag{18}$$

Gut:

$$V_{GB}\, dC_{GB}/dt = Q_G(C_B - C_{GB}) + K_G(C_{GT} - C_{GB}) - V_{m_G} C_{GB}/(K_{m_G} + C_{GB}) \tag{19}$$

$$V_{GT}\, dC_{GT}/dt = K_G(C_{GB} - C_{GT}) + V_{m_G} C_{GB}/(K_{m_G} + C_{GB}) - k_{GL}(C_{GL}/\psi_{GL} - C_{GT}) \tag{20}$$

Gut lumen:

$$V_{GL}\, dC_{GL}/dt = k_{GL}(C_{GL}/\psi_{GL} - C_{GT}) \tag{21}$$

Lung:

$$V_{LuB}\, dC_{LuB}/dt = Q_{Cr} C_{CrB} + Q_K C_{KB} + (Q_{Li} + Q_G) C_{LiB} - Q_B C_{LuB} + K_{Lu}(C_{LuT} - C_{LuB}) - V_{m_{Lu}} C_{LuB}/(K_{m_{Lu}} + C_{LuB}) \tag{22}$$

$$V_{LuT}\, dC_{LuT}/dt = K_{Lu}(C_{LuB} - C_{LuT}) + V_{m_{Lu}} C_{LuB}/(K_{m_{Lu}} + C_{LuB}) \tag{23}$$

Heart:

$$V_H\, dC_{HB}/dt = Q_H(C_B - C_{HB}) + K_H(C_{HT} - C_{HB}) - V_{m_H} C_{HB}/(K_{m_H} + C_{HB}) \tag{24}$$

$$V_{HT}\, dC_{HT}/dt = K_H(C_{HB} - C_{HT}) + V_{m_H} C_{HB}/(K_{m_H} + C_{HB}) \tag{25}$$

Carcass:

$$V_{CrB}\, dC_{CrB}/dt = Q_{Cr}(C_B - C_{CrB}) + K_{CrB}(C_{GR}/\psi_{CrR} - C_{CrB}) \tag{26}$$

$$V_{CrR}\, dC_{CrR}/dt = K_{CrR}(C_{CrB} - C_{CrR}/\psi C_{CrR}) \tag{27}$$

$$V_{CrS}\, dC_{CrS}/dt = K_{CrS}(C_{CrB} - C_{CrS}/\psi_{CrS}) \tag{28}$$

Urine:

$$d(C_u \dot{V}_u)/dt = k_{GF} C_{KB} + V_{m_{TS}} C_{KB}/(K_{m_{TS}} + C_{KB}) \tag{29}$$

APPENDIX III

With each tissue that is represented in the mathematical model, there are at least three diffusional and transport parameters that need to be determined. Simultaneous estimation of 21 independent parameters would lead to a lengthy session of trial and error. An approximation technique was developed to reduce the degrees of freedom for certain parameters. This procedure is demonstrated below using the heart tissue as an example.

The basic equation governing the movement of TEA into the heart tissue was hypothesized to be

$$V_{HT}\,dC_{HT}/dt = K_H(C_{HB} - C_{HT}) + V_{m_H}C_{HB}/(K_{m_H} + C_{HB}) \qquad (30)$$

It is possible to obtain a numerical estimate of the time-dependent variables dC_{HT}/dt, C_{HB}, and C_{HT} at a given time from the single-dose washout data. When these estimates are substituted in the above equation, we have reduced by 1 degrees of freedom for the parameters V_{m_H}, K_H, and K_{m_H}. If this process is repeated with data from another time point (distant from the first time to assume a maximum of independence in the data), the degrees of freedom will be reduced again.

The time at which peak tissue concentration is observed (t_p) and the last sampling time (t_l) were selected because dC_{HT}/dt will be low at both instances, and the data are also taken over a wide range of blood concentrations. For the heart, t_p and t_l are 30 and 300 min, respectively. The variables C_{HT} and C_{HB} are estimated as follows:

C_{HB} is assumed to be equal to C_B since dC_{HT}/dt is low and the organ is well perfused.

C_{HT} is calculated by the equation

$$C'_H = (V_{HT}C_{HT} + V_{HB}C_{HB})/(V_{HT} + V_{HB}) \qquad (31)$$

which is rearranged to give

$$C_{HT} = (C'_H(V_{HT} + V_{HB}) - V_{HB}C_{HB})/V_{HT} \qquad (32)$$

To estimate dC_{HT}/dt at t_l the last three tissue concentration–time points were fitted to the equation

$$C'_H = C^0_H e^{-\beta_H t} \qquad (33)$$

where C^0_H is the extrapolated zero-time tissue concentration and β_H is the exponential rate constant for the decline of tissue concentration vs. time. On differentiation,

$$dC'_H/dt = -(\beta_H C^0_H)\, e^{-\beta_H t} \qquad (34)$$

Table X.

Variable	$t_p = 30$ min	$t_l = 300$ min
C_{HB}, μg/ml	1.3	0.022
C_{HT}, μg/g	11.5	2.76
dC_{HT}/dt, μg/ml/min	0	0.0163

From equation (31)

$$dC_{HT}/dt = [dC'_H/dt(V_{HT} + V_{HB}) - V_{HB} \times dC_{HB}/dt]/V_{HT} \quad (35)$$

The term dC_{HB}/dt can be estimated from the plasma concentration data in a similar manner as described for dC'_H/dt. At t_p, dC'_{HT}/dt is considered to be zero.

The variable estimates for the heart are summarized in Table X. Substituting in equation (12) results in

$$t = 30 \text{ min} \qquad 0 = K_H(1.3 - 11.5) + V_{m_H}(1.3)/(K_{m_H} + 1.3) \quad (36)$$

$$t = 300 \text{ min} \qquad (0.0163)(0.88) = K_H(0.022 - 2.76) + V_{m_H}(0.022)/(K_{m_H} + 0.022) \quad (37)$$

Simplifying these equations,

$$t = 30 \text{ min} \qquad V_{m_H} = K_H(K_{m_H} + 1.3)(7.85) \quad (38)$$

$$t = 300 \text{ min} \qquad V_{m_H} = (K_H + 0.0051)(K_{m_H} + 0.022)(124.5) \quad (39)$$

If the assumption is made that $K_H \gg 0.0051$, then

$$t = 300 \text{ min} \qquad V_{m_H} = K_H(K_{m_H} + 0.022)(124.5) \quad (40)$$

Combining equations 38 and 40,

$$V_{m_H}/K_H = (K_{m_H} + 0.022)(124.5) = (K_m + 1.3)(7.85) \quad (41)$$

or

$$K_{m_H} = 0.064 \ \mu\text{g/ml} \quad (42)$$

The K_{m_H} estimate was substituted in equation 38 to yield

$$V_{m_H}/K_H = 10.71 \ \mu\text{g/ml}$$

Since blood flow is not the rate-limiting factor, i.e., $K_H < Q_H$, as a first approximation one can arbitrarily set $K_H = 0.01Q_H$; therefore,

$$K_H = 0.03 \text{ ml/min}$$

$$V_{m_H} = 0.32 \ \mu\text{g/min}$$

It should be noted that the magnitude of the permeability constant K_i determines how quickly the peak tissue concentration is reached. The larger the estimate of K_i, the shorter the time to peak. On the other hand, the rate of decline of tissue concentration (i.e., the washout) is dependent on the relative magnitude of V_{m_i} and K_{m_i}. These guidelines helped in the parameter adjustments during the computer iteration. While the situation with the other tissues is more complex (e.g., with liver which receives input from the blood compartment as well as the gut compartments), it is always possible to reduce the degrees of freedom using the above approach.

In the case of the heart tissue, our initial estimates of the transport parameters provided an excellent fit of the data. With the other tissues, the final estimates were all well within an order of magnitude of the initial estimates.

REFERENCES

1. K. J. Himmelstein and R. J. Lutz. A review of the applications of physiologically based pharmacokinetic modeling. *J. Pharmacokin. Biopharm.* **7**:127–145 (1979).
2. N. Benowitz, R. P. Forsyth, K. L. Melmon, and M. Rowland. Lidocaine disposition kinetics in monkey and man. II. Effects of hemorrhage and sympathomimetic drug administration. *Clin. Pharmacol. Ther.* **16**:99–109 (1974).
3. R. L. Dedrick. Animal scale-up. *J. Pharmacokin. Biopharm.* **1**:435–461 (1973).
4. H. Shindo, I. Takahashi, and E. Nakajima. Autoradiographic studies on the distribution of quaternary ammonium compounds. II. Distribution of ^{14}C-labelled decamethonium, hexamethonium and dimethonium in mice. *Chem. Pharm. Bull.* **19**:1876–1885 (1971).
5. J. R. Weeks and J. D. Davis. Chronic intravenous cannulas for rats. *J. Appl. Physiol.* **19**:540–541 (1964).
6. L. S. Schanker and A. S. Morrison. Physiological disposition of guanethidine in the rat and its uptake by heart slices. *Int. J. Neuropharmacol.* **4**:27–39, (1965).
7. J. R. Ronbinson. Some effects of glucose and calcium upon the metabolism of kidney slices from adult and newborn rats. *Biochem. J.* **45**:68–74 (1949).
8. K. A. Dandekar and H. B. Kostenbauder. Effect of sodium salicylate on renal elimination of a quaternary ammonium compound. *J. Pharm. Sci.* **66**:56–60 (1977).
9. W. D. Conway, V. K. Batra, and A. Abramowitz. High voltage paper electrophoresis for characterization of drug metabolites. *J. Pharm. Sci.* **62**: 1810–1817 (1973).
10. R. D. Hughes, P. Milburn, and R. T. Williams. Molecular weight as a factor in the excretion of monoquaternary ammonium cations in the bile of the rat, rabbit and guinea pig. *Biochem. J.* **136**:967–978 (1973).
11. C. M. Metzler. *NONLIN: A Computer Program for Parameter Estimation in Nonlinear Situations*, Technical Report 7292/69/7293/005, Upjohn Co., Kalamazoo, Mich. November 25, 1969.
12. M. Gibaldi and D. Perrier. Pharmacokinetics. In J. Swarbrick (ed.), *Drugs and the Pharmaceutical Sciences.* Dekker, New York, 1975, p. 89.
13. P. L. Altman and D. S. Dittmer (eds.), *Biology Data Book*, 2nd ed., Vol. III, Federation of American Scoieties for Experimental Biology, Bethesda, Md., 1974.
14. B. R. Rennick and G. K. Moe. Stop flow localization of renal tubular excretion of tetraethylammonium. *Am. J. Physiol.* **198**:1267–1270 (1960).
15. K. Turnheim and F. O. Lauterbach. Absorption and secretion of monoquaternary ammonium compounds by the isolated intestinal mucosa. *Biochem. Pharmacol.* **26**:99–108 (1977).

16. J. Holm. Transport and exchange of tetraethylammonium in mouse kidney cortical slices. *Biochem. Pharmacol.* **27:**999–1003 (1978).
17. B. Rennick, B. Hamilton, and R. Evans. Development of renal tubular transports of TEA and PAH in the puppy and piglet. *Am. J. Physiol.* **201:**743–746 (1961).
18. P. L. Altman and D. S. Dittmer (eds.), *Biological Handbooks—Blood and Other Body Fluids*, Federation of American Societies for Experimental Biology, Washington, D.C. 1961.
19. K. B. Bischoff, R. L. Dedrick, D. S. Zaharko, and J. A. Longstreth. Methotrexate pharmacokinetics., *J. Pharm. Sci.* **60:**1128–1133 (1971).
20. T. G. Coleman, R. D. Manning, Jr., R. A. Norman, Jr., and A. C. Guyton. Dynamics of water isotope distribution. *Am. J. Physiol.* **223:** 1371–1375 (1972).
21. R. M. Levine, M. R. Blair, and B. B. Clark. Factors influencing the intestinal absorption of certain monoquaternary anticholinergic compounds with special reference to benzomethamine [*N*-diethylaminoethyl-*N'*-methyl-benzilamide methobromide (MC-3199)]. *J. Pharmacol. Exp. Ther.* **114:**78–86 (1955).
22. F. B. Hildebrand. *Introduction to Numerical Analysis.* 2nd ed., McGraw-Hill, New York, 1974, p. 252.
23. A. Rescigno and G. Segre. *Drug and Tracer Kinetics*, 1st ed. (American), Blaisdell, Waltham, Massachusetts, 1966, p. 91.
24. G. Levy and M. Gibaldi. Pharmacokinetics. In O. Eichler, A. Farah, H. Herken, A. D. Welch, (eds.), *Handbook of Experimental Pharmacology*, Vol. XXVIII/3, Springer–Verlag, New York, 1975, p. 19.
25. K. A. Pittman and G. A. Portmann, Pharmacokinetics of pentazocine in the rhesus monkey. *J. Pharm. Sci.* **63:**84–88 (1974).
26. L. L. Miller. Physiological factors and liver cell function. *J. Histochem. Cytochem.* **7:**235–236 (1959).
27. G. Barber-Riley. Uptake of bromosulphthalein by incubated rat liver slices. *S. Afr. J. Med.* **26:**91–97 (1961).
28. C. D. Thron. Some remarks on compartment analysis of uptake and washout data. *Life Sci.* **22:**1287–1304 (1978).